

NUCLEAR MATERIALS TESTING IN THE LOOPS OF THE NRU RESEARCH REACTOR USING MATERIAL TEST BUNDLES

T.C. Leung & L. Walters
AECL Chalk River Laboratories, Chalk River
Ontario, CANADA KOJ 1J0
leungt@aecl.ca watersl@aecl.ca

Abstract

The NRU research reactor has been used to obtain data to understand and quantify the effects of irradiation on nuclear reactor components through their in-service lives and to develop improved designs and components. Apart from the Mark-4 and Mark-7 fast neutron rod material testing facilities in NRU, the high-pressure/high-temperature experimental loops provide an environment similar to the CANDU reactor core, where test materials are subjected to simulated power reactor conditions. Nuclear materials are tested in the loops using Material Test Bundles (MTB). This paper describes how the MTB is designed to operate in the NRU loops. It also describes the physics calculation of the 89-energy-group neutron spectrum in the MTB and its comparison with the spectrum in CANDU power reactors. The predictions of spectral effects on nuclear material behaviour, such as material damage and helium generation are summarized.

1. Introduction

The National Research Universal (NRU) reactor at Chalk River began operation in 1957. It is used to carry out research in basic science and in support of the CANDU power reactor programs, such as the fuel bundle and material development programs. It is also a major supplier of medical radioisotopes in Canada and the world. The NRU reactor is heavy water cooled and moderated, with on-line refueling capability. It is licensed to operate at a maximum power of 135 MW, and has a peak thermal neutron flux of approximately $4.0 \times 10^{18} \text{ n}\cdot\text{m}^{-2}\cdot\text{s}^{-1}$. Figure 1 shows an NRU core lattice, with 31 rows and 18 columns (A to S, with no column “T” and not to be confused with “1”). The hexagonal lattice pitch is 19.685 cm (7-3/4 inch).

The NRU research reactor has been used to obtain data to understand and quantify the effects of irradiation on nuclear reactor components through their in-service lives and to develop improved designs and components. Materials of specific interest are zirconium and its alloys, which are used in the pressure tubes and calandria tubes of CANDU reactors. Various in-reactor material test programs have been conducted in NRU for many years, including experiments on irradiation-induced creep and growth, on corrosion and on fracture properties. In general, displacement of atoms due to irradiation can occur through a variety of processes. The two main processes that apply to materials in the core of a power reactor are (i) atom displacement and cascade from direct neutron collisions, and (ii) thermal neutron capture and subsequent gamma, proton and alpha particle release coupled with atomic recoil. The displacement damage that affects the in-core zirconium alloy material properties is caused primarily by direct fast neutron collisions.

Recently, there is a need for the testing of materials which are also sensitive to the lower energy portion of the neutron spectrum. For example, the Inconel X-750 components in the garter springs of the CANDU reactor contain ~70% Ni and are distinct in that absorption of thermal neutrons by the most abundant isotope Ni-58 produces Ni-59, which has three highly exothermic reactions: (n,α), (n,γ), (n,p). These reactions contribute to displacement damage and the generation of significant amounts of helium and hydrogen. Experimental investigations into the effects of irradiation damage on this material will be performed in the NRU reactor.

This paper describes how the material test bundle (MTB) is designed to operate in the NRU loops. It also describes the physics calculation of the 89-energy-group neutron spectrum in the MTB and its comparison with the spectrum in CANDU power reactors. The use of the MTB neutron spectra for nuclear material behaviour predictions, such as material damage and helium generation is summarized.

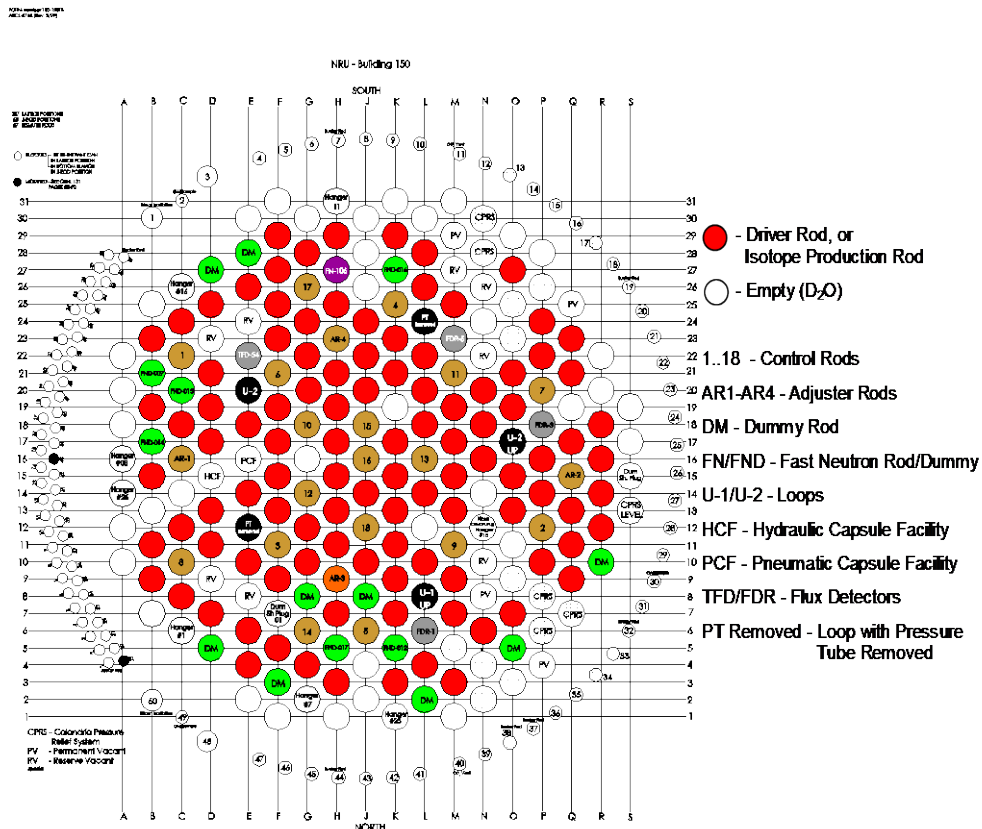


Figure 1 The NRU Core Lattice

2. Materials Testing in the NRU Loops Using Material Test Bundles

Apart from the Mark-4 and Mark-7 fast neutron rod material testing facilities in NRU, the high-pressure/high-temperature experimental loops provide an environment similar to the CANDU reactor core, where test materials are subjected to simulated power reactor conditions. Nuclear materials are tested in the loops using MTBs. The MTB is designed to enable metallurgical specimens to be irradiated in a high-flux position in an NRU loop, such as the two middle positions on a loop fuel string, as shown in Figure 2. The NRU loops are high temperature and high pressure test facilities, in which test elements may be subjected to conditions simulating those existing in power reactors. The loop test section is confined to a 10.3 cm ID pressure tube, made of Zr 2.5% Nb. The design pressure of the U-1 and U-2 loops is 13.8 MPa. For the U-2 loop, it is in a U-shape with two sections. The flow at the inlet section at site E20 is down, while the flow at the outlet section at site O17 is up. The loops and the fuel bundles are both cooled by light water. The MTB is a 30-element bundle, similar to a 37-element CANDU fuel bundle with the 7 centre elements removed, as shown in Figure 3a. The overall length of the MTB is 482 mm. Its outer fuel ring has 18 elements with uranium enriched to 1.25 wt% U-235, and its inner ring has 12 elements with uranium enriched to 1.7 wt% U-235. The centre seven elements of the bundle are replaced by a 41.7 mm ID, 43.2 mm OD Zircaloy tube welded to the webs of the end plates. The tube provides internal support for the bundle and serves as a guide for the specimen holder assembly, which varies for different experiments depending on the sample requirements.

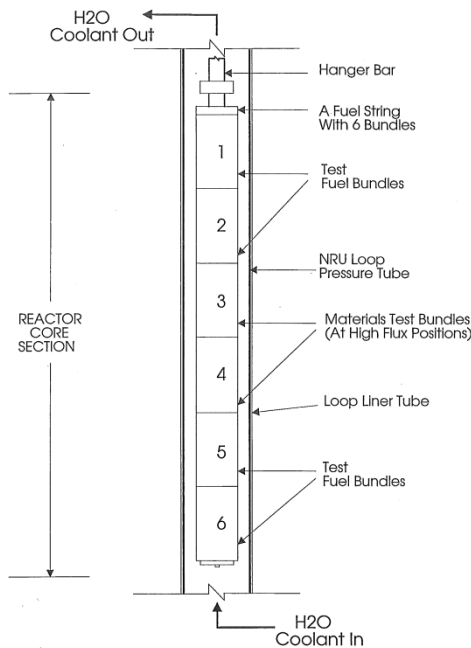


Figure 2 Material Test Bundles in a Loop Site.

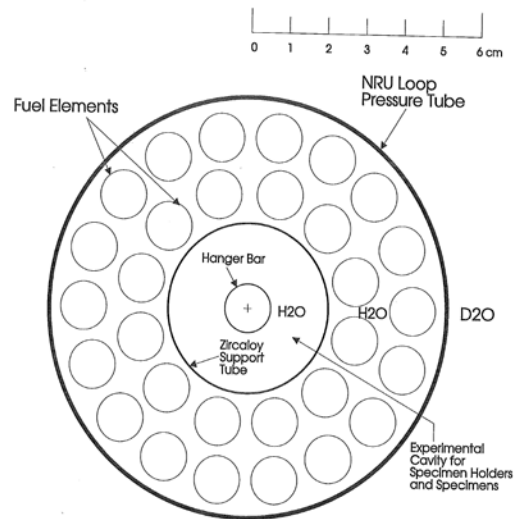


Figure 3a A Material Test Bundle.

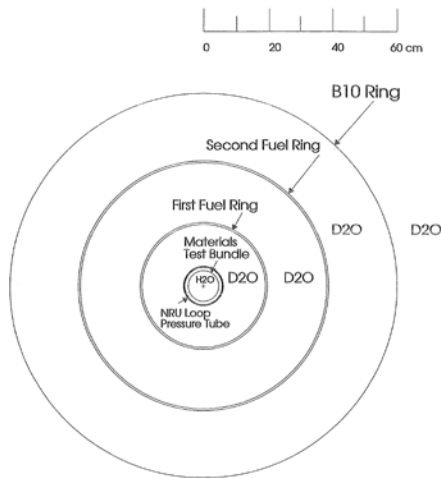


Figure 3b Sketch of the Super-cell model for the MTB analysis.

3. Method of Calculation of the 89-Group Neutron Spectra

Calculations of the neutron flux spectra in the experimental cavities of the MTB were performed using the WIMS-AECL code [1], which is a multi-group transport code with two-dimensional capabilities using the “Pij” collision probability method. The main transport calculations were performed using 89 energy groups. For the neutron spectrum calculation, the version of WIMS-AECL used was version 2.5d, and the older data library of ENDFB/V was used, so that the calculation method was the same as with the rest of the NRU assemblies. In the future the neutron spectra could be re-calculated using a newer version of WIMS-AECL, such as 3.1, and newer data libraries, ENDFB/VI or /VII. It is expected that variation of the calculation results using a different version of WIMS-AECL and different data libraries would be small, based on previous calculation results from other NRU sites.

The experimental section of the material testing facility was modeled as a super-cell, which included the cell-of-interest and a representation of its environment (see Figure 3b). The neighbouring fuel rods provide the correct driving spectrum for the MTB, and are modeled as two fuel rings located at radii of 20.2 cm and 39.9 cm from the centre of the cell. The fuel loading in these two rings was about 2.39 g/cm and 4.34 g/cm of U-235. An adjustable boron-10 ring was added outside the fuel rings, in order to keep the k-effective close to 1.000 throughout the burnup range.

The experimental insert was modeled as four annuli: the first for the centre hanger bar, the second and the third for the specimen holder and specimens, and the fourth for the enclosing zircaloy support tube. The radii and material composition of the second and third annuli may vary slightly, depending on the types of specimens and specimen holders were used.

The operating flux and power of the MTB in an NRU core configuration are calculated using the TRIAD code [3]. The MTB neutron fluxes are normalized to a nominal flux of

$2.85 \times 10^{18} \text{ n}\cdot\text{m}^{-2}\cdot\text{s}^{-1}$, in the first driver-fuel ring. This is equivalent to normalizing to a linear bundle fission power of 1.73 MW/m, or a total bundle fission power of approximately 834 kW. The linear fission powers of the fuel elements in the inner and outer fuel rings of the MTB are 58.5 and 57.1 kW/m, respectively.

4. Results of the MTB Neutron Spectra Calculations

4.1 The MTB Neutron Spectra

In assessing the total material damage, the total fluxes for the whole energy spectrum are required. Table 1 lists the WIMS calculated neutron fluxes at the specimen irradiation location inside the experimental cavity of the MTB in the NRU Loops. The neutron flux is usually highest at the U-2 up leg at the O-17 site. Because some CANDU reactor materials, such as the Inconel garter spring, will experience damage from both fast and thermal neutrons (see Sec. 5), Table 1 lists details of the neutron spectrum for both the fast energy groups ($E > 1.05 \text{ MeV}$) and the thermal energy groups below 0.625 eV. The fast neutron flux above 1.05 MeV in the experimental cavity of the MTB is $5.31 \times 10^{17} \text{ n}\cdot\text{m}^{-2}\cdot\text{s}^{-1}$, the thermal neutron flux below 0.625 eV at the same location is $1.22 \times 10^{18} \text{ n}\cdot\text{m}^{-2}\cdot\text{s}^{-1}$, and the total neutron flux is $3.40 \times 10^{18} \text{ n}\cdot\text{m}^{-2}\cdot\text{s}^{-1}$. In percentages, the fast neutron flux above 1.05 MeV is 15.61% of the total, and the thermal flux is 35.96%.

4.2 Comparison of Neutron Spectra in the Fast Neutron Rods and MTB in NRU with CANDU Reactor

The comparisons of the neutron spectra in the fast neutron rods and MTB in NRU and in the CANDU pressure tube locations are shown in Table 1 and also graphically shown in Figure 4. Each neutron spectrum is normalized to its own total fluxes, for example, 3.40, 3.44, 5.19, and $3.18 \times 10^{18} \text{ n}\cdot\text{m}^{-2}\cdot\text{s}^{-1}$ for the MTB, CANDU, Mk7 and Mk4 fast-neutron rod total fluxes, respectively. The CANDU fluxes were calculated using WIMS-AECL, version 3.1.2 at pressure tube locations for an average power fuel channel with mid-burnup fuel. The percentages of fast/thermal fluxes of the total fluxes for the MTB, CANDU, Mk7 and Mk4 fast-neutron rods are 15.61%/35.96%, 7.22%/54.70%, 13.09%/39.58%, and 6.47%/65.15%, respectively.

In the thermal neutron energy range in Figure 4, the MTB fluxes are lower than the CANDU fluxes and the Mk7 and Mk4 rod fluxes, while in the epi-thermal neutron energy range, the MTB fluxes coincide with the CANDU fluxes. In the fast flux ($E > 1 \text{ MeV}$) energy range, the flux in the MTB is greater than that in the CANDU pressure tube.

Table 1 Comparisons of Fast and Thermal Neutron Spectra inside the Material Testing Facilities in NRU and in the CANDU Reactor.

Group	Energy Width (MeV)	MTB Flux ($\times 10^{16}$ $n \cdot m^{-2} \cdot s^{-1}$)	MTB Flux (% of total)	CANDU PT Flux ($\times 10^{16}$ $n \cdot m^{-2} \cdot s^{-1}$)	Mk 7 Rod Flux ($\times 10^{16}$ $n \cdot m^{-2} \cdot s^{-1}$)	Mk 4 Rod Flux ($\times 10^{16}$ $n \cdot m^{-2} \cdot s^{-1}$)
1	7.79-10.0	0.422	0.124	0.212	0.573	0.176
2	6.07-7.79	1.188	0.349	0.611	1.593	0.500
3	4.72-6.07	2.682	0.789	1.370	3.584	1.114
4	3.68-4.72	4.488	1.320	2.230	6.007	1.814
5	2.87-3.68	6.777	1.993	3.240	8.926	2.713
6	2.23-2.87	8.957	2.634	4.340	11.633	3.580
7	1.74-2.23	9.021	2.653	4.170	11.743	3.469
8	1.35-1.74	9.830	2.891	4.450	12.259	3.676
9	1.05-1.35	9.716	2.857	4.230	11.728	3.541
Fast $E > 1.05$ MeV	Sub-total	53.080	15.609	24.853	68.045	20.584
Epi-thermal	0.625×10^{-6} -1.05	164.706	48.434	131.018	245.957	90.266
66	$(0.5-0.625) \times 10^{-6}$	1.745	0.513	1.620	1.367	2.735
67	$(0.4-0.5) \times 10^{-6}$	2.034	0.598	1.690	1.414	2.779
68	$(0.35-0.4) \times 10^{-6}$	1.510	0.444	1.080	0.880	1.693
69	$(0.32-0.35) \times 10^{-6}$	1.227	0.361	0.763	0.616	1.158
70	$(0.3-0.32) \times 10^{-6}$	1.031	0.303	0.586	0.467	0.856
71	$(0.28-0.3) \times 10^{-6}$	1.281	0.377	0.688	0.539	0.956
72	$(0.25-0.28) \times 10^{-6}$	2.537	0.746	1.350	0.998	1.664
73	$(0.22-0.25) \times 10^{-6}$	3.622	1.065	2.050	1.412	2.124
74	$(0.18-0.22) \times 10^{-6}$	7.465	2.195	4.960	3.348	4.352
75	$(0.14-0.18) \times 10^{-6}$	12.521	3.682	10.500	7.859	8.807
76	$(0.10-0.14) \times 10^{-6}$	20.309	5.972	22.800	20.216	20.596
77	$(0.08-0.10) \times 10^{-6}$	13.774	4.050	19.700	19.289	19.696
78	$(0.067-0.08) \times 10^{-6}$	10.057	2.957	16.800	17.311	18.014
79	$(0.058-0.067) \times 10^{-6}$	7.326	2.154	13.700	14.570	15.322
80	$(0.05-0.058) \times 10^{-6}$	6.637	1.952	13.500	14.804	15.695
81	$(0.042-0.05) \times 10^{-6}$	6.594	1.939	14.600	16.429	17.532
82	$(0.035-0.042) \times 10^{-6}$	5.573	1.639	13.300	15.429	16.565
83	$(0.030-0.035) \times 10^{-6}$	3.764	1.107	9.570	11.352	12.244
84	$(0.025-0.03) \times 10^{-6}$	3.494	1.027	9.360	11.317	12.249
85	$(0.02-0.025) \times 10^{-6}$	3.134	0.922	8.830	10.907	11.844
86	$(0.015-0.02) \times 10^{-6}$	2.672	0.786	7.900	9.986	10.874
87	$(0.01-0.015) \times 10^{-6}$	2.093	0.615	6.450	8.391	9.160
88	$(0.005-0.01) \times 10^{-6}$	1.377	0.405	4.380	5.899	6.448
89	$(0.002-0.005) \times 10^{-6}$	0.502	0.148	1.620	2.269	2.480
Thermal	Below 0.625×10^{-6}	122.280	35.958	188.180	205.672	207.238
Total		340.065	100.000	344.051	519.674	318.090

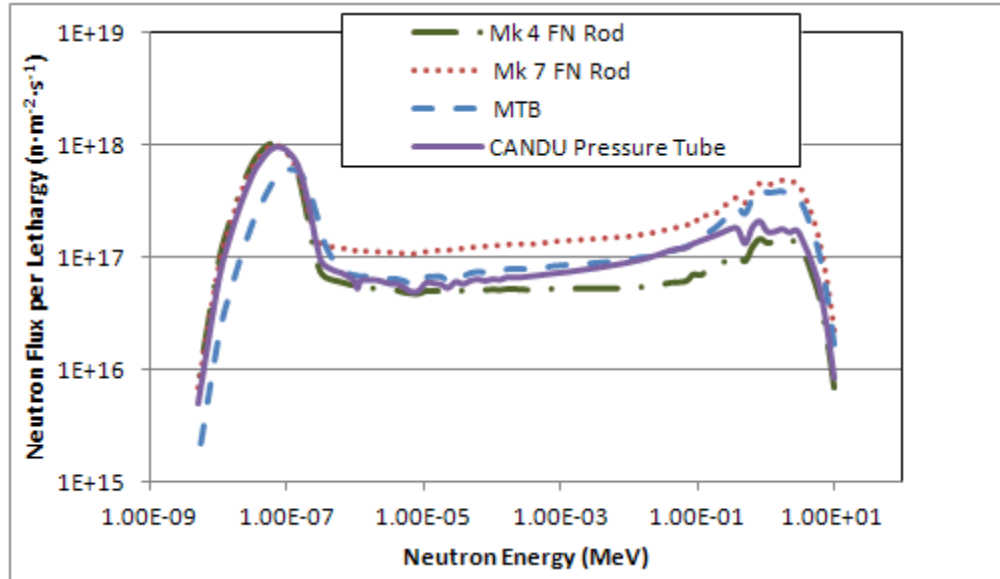


Figure 4 Flux per lethargy vs. Neutron energy

The MTB total flux in NRU is lower than the total fluxes in many other material test reactors (MTRs) outside Canada, which means that NRU is not optimum for end-of-life materials studies; however, a low flux is ideal to study stress relaxation and transient phenomena where the majority of the changes to the material are occurring over relatively low doses ($\sim 1 \times 10^{25} \text{ n} \cdot \text{m}^{-2}$). Also, since the flux levels are similar to CANDU, performing materials irradiation tests in NRU rather than in a high flux MTR eliminates the possibility of introducing different rate-dependent changes in point defect concentrations and their effects on vacancy-interstitial recombination rates.

5. Use of the MTB Neutron Spectra for Material Test Predictions

In the core of a nuclear reactor, most of the atomic displacement damage that gives rise to enhanced creep is caused primarily by direct collisions of fast neutrons with atoms in the components. The damage process follows several stages. In a single crystal of zirconium, the displacement energy of the crystal lattice needs a threshold energy of an incoming neutron to cause damage. A zirconium atom is about ninety times the mass of a neutron. Thus, if the **primary knock-on zirconium atom** (PKA) is bound to the lattice by 40 eV, the minimum energy of a neutron that can cause displacement by a direct collision must be $\sim 1 \text{ keV}$. Neutron energies below this threshold cannot displace zirconium nuclei from lattice positions and hence no mobile zirconium interstitials are created. The 40 eV value for zirconium is the recommended value of the effective displacement energy for use in displacement calculations by the ASTM, American Society for Testing and Materials [4].

If the neutron energy is above the threshold displacement energy, the recoil energy of the PKA is transferred to nearby zirconium nuclei. The PKA is charged and thus partially slowed by electrical repulsion leading to heat. However, much of its energy is transferred

by direct collision to nearby zirconium nuclei which, in turn, recoil and are displaced from their lattice positions. Each zirconium nuclei is able to participate in secondary collisions. A collision cascade develops that can involve hundreds of displaced atoms, the number depending on the initial PKA recoil energy. This cascade happens in a very short time. Once the cascade forms, the internal electrical forces amongst defects and the temperature dependence of interstitial diffusion cause most of the mobile interstitials to recombine at a nearby lattice vacancy. It is estimated that up to 10% of the displaced atoms never find their way back to a lattice position.

The current method for determining radiation damage is to obtain calculated neutron spectrum data and then compute the relative damage rates using compatible damage cross sections. The cross sections describe the relative probability of causing an atomic displacement. Therefore, the chance of a nuclear reaction is described by a set of multigroup fluxes (ϕ_g in $n/cm^2/s$) combined with a set of energy-dependent neutron damage cross sections (σ_g in $eV\text{-}cm^2$), which are determined and processed like other nuclear cross sections [5]. The damage rate, R , in eV/s for an atom density of (Σ_g in cm^{-1}), is computed as:

$$R = \sum_g \phi_g \sigma_g$$

where the sum is over all energy groups, g .

The damage cascade caused by a head-on collision between a zirconium nucleus and a fast neutron of incident energy 1 MeV may contain up to 400 displaced atoms. Thus, the rate for the displacement per atom (dpa) can be determined from the damage rate R [5,6]. Using the SPECTER code [7] to determine damage in the material, Figure 5 shows a comparison of the dpa generated in Zr-2.5Nb CANDU pressure tube materials using the spectra shown in Figure 4.

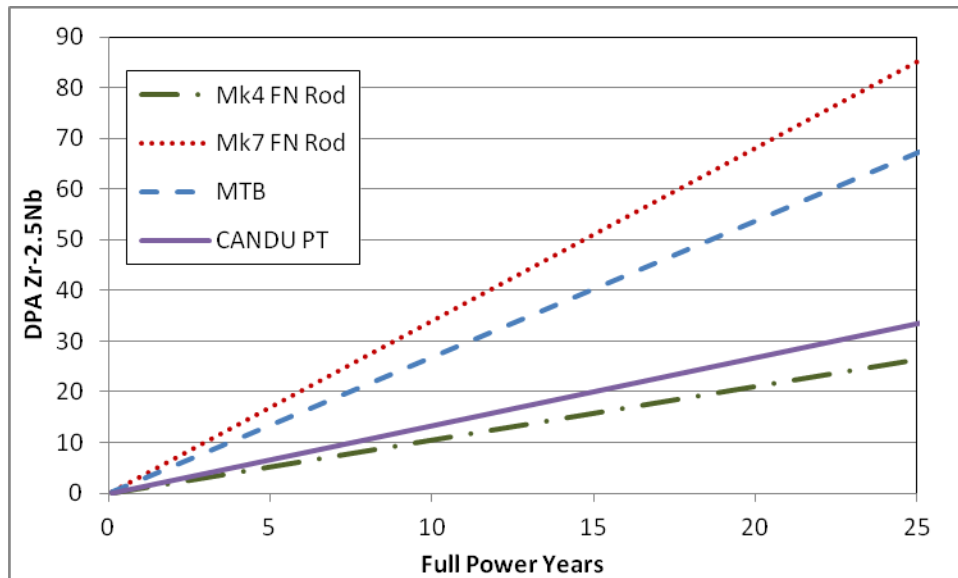
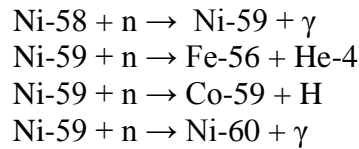


Figure 5 DPA for Zr-2.5Nb Material in NRU and in a Maximum Power CANDU Pressure Tube

Using dpa from fast neutrons is valid for comparison of data from various spectral environments only if no other process is acting strongly. Displacements caused by thermal neutrons in a CANDU reactor core can usually be neglected, especially for zirconium components. However, for components containing natural nickel neutron absorption at thermal energies will cause the following transmutations.



Therefore, Inconel garter springs (which contain ~70% Ni) will experience damage from all energies including fast neutrons ($E > 1\text{MeV}$) and thermal neutrons ($E < 0.625\text{ eV}$). Transmutation of Ni-58 to Ni-59 with subsequent (n,p) and (n, α) processes produces a significant additional component to the total damage. Although the ejected particles cause displacements, by far the biggest contribution to the displacement per event is the atom recoil. Details of the damage production for the (n, α), (n,p) and (n, γ) reactions are given in [8,9].

For Ni-58, the minimum neutron energy needed to cause direct displacement damage is 580 eV when the atomic displacement threshold energy is 40 eV. The isotope Ni-59 has relatively high thermal neutron capture cross section which enables the production of helium and hydrogen [8,9]. Since Ni-59 does not exist in natural nickel, it is only generated from the thermal neutron capture reaction. For the (n, α) reaction with Ni-59 the total damage energy is 176.2 keV per neutron capture and therefore the subsequent total number of displacements per neutron capture in Ni-59 is 1762 [8]. Figures 6 and 7 show results for helium generation and dpa for Inconel X-750 material at the garter spring position in CANDU and in NRU. In a CANDU reactor at the garter spring location the dpa from the production of He-4 is larger than from fast neutron damage, as shown in Table 2. Since the MTB has a lower thermal neutron energy flux than the NRU Mk4 and 7 FN rods, the amount of helium generated in a Nickel based alloy will be lowest among these NRU facilities. However, the total dpa produced in the MTB will be similar to that produced in the Mk4 FN rod due to the higher fast flux range of the neutron spectrum.

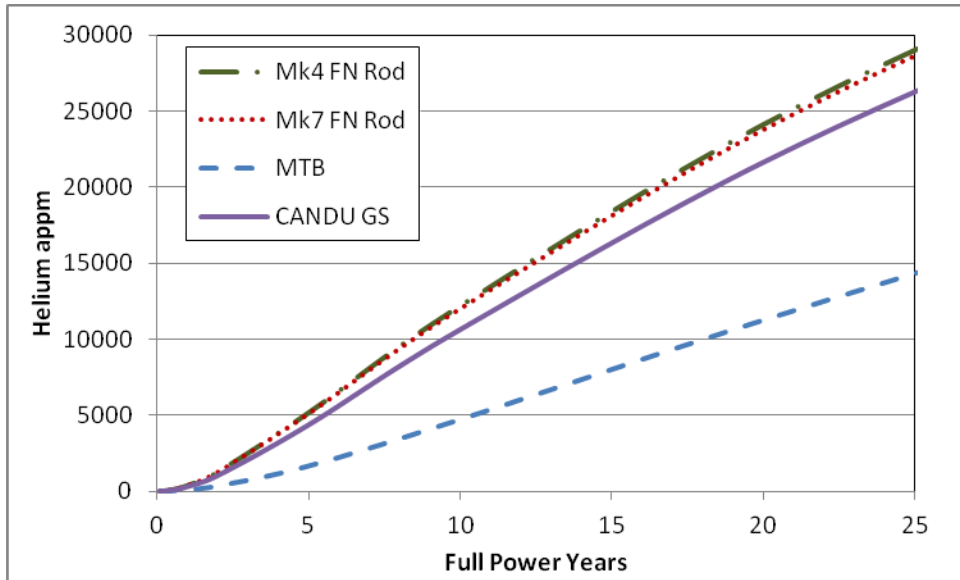


Figure 6 Helium Generated in Inconel X-750 Material in NRU and at the CANDU Garter Spring Location. (“appm” is the atom parts per million).

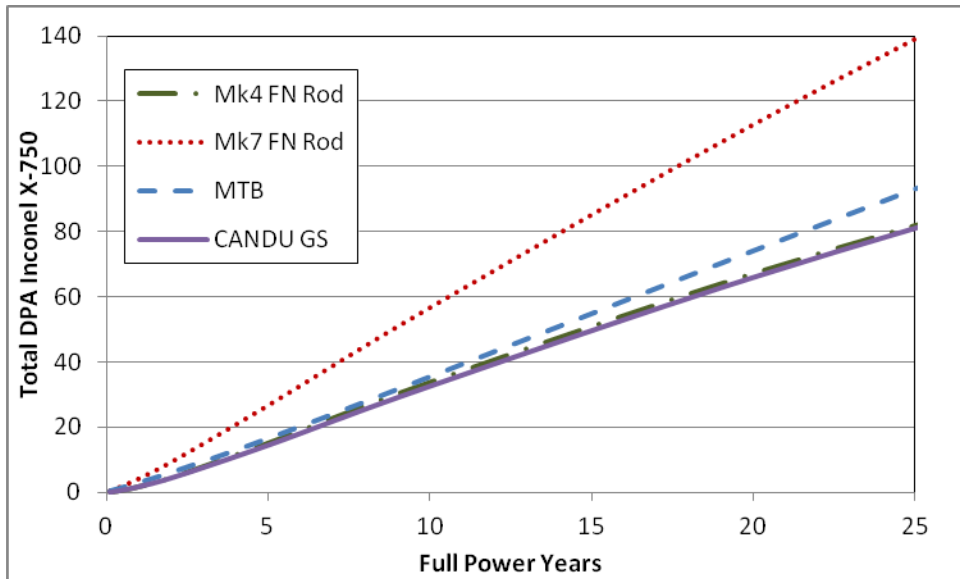


Figure 7 Total DPA in Inconel X-750 Material in NRU and at the CANDU Garter Spring Location.

Table 2 summarizes displacement rates for Zr-2.5Nb and X-750 materials in NRU and in CANDU. For in-reactor components containing natural nickel not only is there a contribution to displacements caused by atom recoil associated with photon emission, but more significantly the process of transmutation giving Ni-59 is a major contributor to the damage process. Table 2 shows that while dpa from direct displacement is similar for Zr-Nb and Inconel X-750 materials, the total dpa for Inconel X-750 materials is notably larger due to the contribution from the Ni-59 (n,α) reactions. Based on Figure 7 and

Table 2, the Mk4 neutron rod seems better suited for simulating the DPA in a CANDU pressure tube than the MTB, but the MTB has a higher total flux, and it provides a better “accelerated” test to achieve the same neutron integrated flux (fluence) faster. In addition, because the MTB has the same testing conditions of temperature and pressure as the CANDU pressure tube, it provides useful testing results for coolant corrosion.

Table 2 Calculated DPA after 25 years irradiation for Zr-2.5Nb and X-750 Test Materials in NRU and in an average Power CANDU Channel

	MTB in NRU	Mk4 FN Rod in NRU	Mk7 FN Rod in NRU	CANDU
dpa from direct displacement in X-750 material	67	29	88	33
dpa from Ni-59 (n, α) in X-750	26	53	52	48
dpa from direct displacement in Zr-2.5Nb material	67	26	86	34

6. Conclusions

Several conclusions can be drawn from the use of the MTB in NRU loops for nuclear material testing.

- 1) AECL at Chalk River can provide opportunities for material testing in the NRU loops using the MTB, under a test condition similar to that of the CANDU operating condition. Material tests are not limited to damage due to fast neutrons, but also include material tests that are sensitive to the thermal neutrons.
- 2) The 89-group energy spectra for the MTB were calculated using WIMS-AECL code, and the overall energy spectra are similar to those of the CANDU reactors. In the thermal neutron energy range, the CANDU fluxes are slightly higher than the MTB fluxes, while in the fast neutron energy range, the fluxes in the MTB are larger.
- 3) Based on the calculated 89-group energy spectra, material damage due to neutron irradiation and helium production were predicted. Material test results from the MTB in the NRU loops will be directly applicable in determining materials behavior in CANDU reactors.

7. Acknowledgements

The authors would like to thank M. Griffiths from AECL and L. R. Greenwood from Pacific Northwest National Laboratory for their guidance and assistance with the assessment of spectral effects on material behavior. The authors are also thankful to J. Pencer for providing the CANDU neutron spectrum at the pressure tube location.

8. References

- [1] J.D. Irish and S.R. Douglas, "Validation of WIMS-IST", Proceedings of the 23rd Annual Conference of the Canadian Nuclear Society, Toronto, Canada, 2002 June.
- [2] S.R. Douglas, "A calculational model for the NRU reactor", Paper presented at the Canadian Nuclear Society 1985 Annual Conference; also AECL Report, AECL-8841, 1985 June.
- [3] T.C. Leung and M.D. Atfield, "Validation of the TRIAD3 Code Used for the Neutronic Simulation of the NRU Reactor", Proceedings of the 30th Annual Conference of the Canadian Nuclear Society, Calgary, Alberta, Canada, 2009 May 31 - June 3.
- [4] D.G. Doran and N.J. Graves, "Neutron Displacement Damage Cross Sections for Structural Metals", Irradiation Effects on the Microstructure and Properties of Metals, ASTM STP 611, American Society for Testing and Materials, 1976, pp. 463-482.
- [5] R.E. MacFarlane and D.W. Muir, "The NJOY Nuclear Data Processing System", Versions 91, 97 and 99, Chapter VI. HEATR, pages 1-45.
- [6] M.J. Norgett, M.T. Robinson, I.M. Torrens, "A Proposed Method of Calculating Displacement Dose Rates", Nuclear Engineering and Design 33 (1975), pp. 50-54.
- [7] L.R. Greenwood and R.K. Smither, "SPECTER: Neutron Damage Calculations for Materials Irradiations", ANL/FPP/TM-197, Argonne National Laboratory, 1985.
- [8] L.R. Greenwood, "A new calculation of Thermal Neutron Damage and Helium Production in Nickel", Journal of Nuclear Materials 115 (1983), pp. 137-142.
- [9] L.R. Greenwood and F.A. Garner, "Hydrogen Generation arising from the ⁵⁹Ni(n,p) Reaction and its impact on Fission-Fusion Correlations", Journal of Nuclear Materials 233-237 Part 2 (1996), pp. 1530-1534.